Contents lists available at ScienceDirect

Acta Biomaterialia

journal homepage: www.elsevier.com/locate/actabiomat

Full length article

Cell-instructive pectin hydrogels crosslinked via thiol-norbornene photo-click chemistry for skin tissue engineering

Rúben F. Pereira [a,b,c,d], Cristina C. Barrias [a,b,c], Paulo J. Bártolo [e,f,*], Pedro L. Granja [a,b,c,g,*]

[a] i3S – Instituto de Investigação e Inovação em Saúde, Universidade do Porto, 4200-135, Portugal
[b] INEB – Instituto Nacional de Engenharia Biomédica, Universidade do Porto, 4200-135, Portugal
[c] ICBAS – Instituto de Ciências Biomédicas Abel Salazar, Universidade do Porto, 4050-343, Portugal
[d] CDRSP – Centre for Rapid and Sustainable Product Development, Polytechnic Institute of Leiria, 2430-028, Portugal
[e] School of Mechanical, Aerospace and Civil Engineering, University of Manchester, M13 9PL, UK
[f] Manchester Institute of Biotechnology, University of Manchester, M1 7DN, UK
[g] FEUP – Faculdade de Engenharia da Universidade do Porto, 4200-464, Portugal

ARTICLE INFO

ABSTRACT

Cell-instructive hydrogels are attractive for skin repair and regeneration, serving as interactive matrices to promote cell adhesion, cell-driven remodeling and *de novo* deposition of extracellular matrix components. This paper describes the synthesis and photocrosslinking of cell-instructive pectin hydrogels using cell-degradable peptide crosslinkers and integrin-specific adhesive ligands. Protease-degradable hydrogels obtained by photoinitiated thiol-norbornene click chemistry are rapidly formed in the presence of dermal fibroblasts, exhibit tunable properties and are capable of modulating the behavior of embedded cells, including the cell spreading, hydrogel contraction and secretion of matrix metalloproteases. Keratinocytes seeded on top of fibroblast-loaded hydrogels are able to adhere and form a compact and dense layer of epidermis, mimicking the architecture of the native skin. Thiol-ene photocrosslinkable pectin hydrogels support the *in vitro* formation of full-thickness skin and are thus a highly promising platform for skin tissue engineering applications, including wound healing and *in vitro* testing models.

Statement of Significance

Photopolymerizable hydrogels are attractive for skin applications due to their unique spatiotemporal control over the hydrogel formation. This study reports the design of a promising photo-clickable pectin hydrogel which biophysical and biochemical properties can be independently tailored to control cell behavior. A fast method for the norbornene-functionalization of pectin was developed and hydrogels fabricated through UV photoinitiated thiol-norbornene chemistry. This one-pot click reaction was performed in the presence of cells using cell-adhesive and matrix metalloproteinase-sensitive peptides, yielding hydrogels that support extensive cell spreading. Keratinocytes seeded on top of the fibroblast-loaded hydrogel formed a compact epidermis with morphological resemblance to human skin. This work presents a new protease-degradable hydrogel that supports *in vitro* skin formation with potential for skin tissue engineering.

1. Introduction

Skin wound healing is a complex, orchestrated cascade of biological processes that rely on the interaction between several mediators, such as extracellular matrix (ECM) molecules, cells, growth factors, cytokines and chemokines, towards the replacement of lost tissue [1]. Despite the variety of commercially available products and therapeutic strategies for skin wound healing (e.g., skin substitutes, wound dressings), the formation of

* Corresponding authors at: School of Mechanical, Aerospace and Civil Engineering, University of Manchester, M13 9PL, UK (Paulo J. Bártolo), i3S – Instituto de Investigação e Inovação em Saúde, Universidade do Porto, 4200-135, Portugal (Pedro L. Granja).

E-mail addresses: paulojorge.dasilvabartolo@manchester.ac.uk (P.J. Bártolo), pgranja@i3s.up.pt (P.L. Granja).

functional skin remains a major challenge [1–3]. Hydrogels are widely explored as templates for skin wound healing due to their chemical versatility, hydrated nature, elasticity and ability to conform into complex-shaped defects. In addition, hydrogels can be designed to provide instructive environments for tissue formation as well as to deliver cells and growth factors in order to stimulate skin regeneration [4–6]. Cell-instructive hydrogels play a pivotal role in tissue engineering due to their biochemical and biophysical similarities with the native ECM, along with the ability to influence the behavior of embedded cells [7,8]. Synthetic materials have been widely explored to design such bioactive hydrogels as they provide greater control over the chemical composition and materials properties [9,10]. However, materials derived from natural sources possess unique features (e.g., cell remodeling, biological recognition, biodegradation) that also make them suitable candidates to engineer ECM analogues [11,12].

Pectin, a structural polysaccharide extracted from the primary cell wall of plants, is receiving increased attention for tissue engineering due to its water solubility, biocompatibility, biodegradability and anionic nature [13–15]. It is a branched polymer composed of multiple polysaccharide domains, providing a multitude of target sites for chemical modification. In addition, pectin hydrogels are susceptible to *in vitro* and *in vivo* degradation [16,17], which is useful for tissue engineering applications. A distinctive characteristic of pectin compared to other bioactive natural polymers (e.g., gelatin, fibrin) relies on the lack of endogenous cell-adhesive and cell-proteolytic sites. This feature allows for the precise introduction of specific biochemical moieties onto the otherwise bioinert polymer backbone [16] in order to control cell fate and to decouple their effect on cell behavior.

The selection of suitable chemistries is of critical importance for the formation of cellularized ECM-inspired polymer hydrogels under cytocompatible conditions, without yielding toxic byproducts. Bio-orthogonal click chemistries assume a central role on the modular synthesis of advanced cell-laden hydrogels, as they can develop under mild conditions in the presence of cells, proceed with high yield and be easily controlled by selecting complementary chemical functionalities [18,19]. Photoinitiated thiol-norbornene chemistry is a click reaction between multifunctional norbornene-modified macromers and sulfhydryl-containing linkers (e.g., dithiothreitol, biscysteine peptides), triggered by UV or visible light in the presence of a low photoinitiator concentration [10]. In contrast to chain-growth hydrogels formed by radical-mediated polymerization, which often contain heterogeneous and high molecular weight crosslinks, light-mediated thiol-norbornene polymerization is non-oxygen inhibited and proceeds through a step-growth mechanism. Hydrogels formed by thiol-norbornene chemistry contain networks with less heterogeneities and lead to the formation of engineered tissues with improved overall quality [20,21]. Furthermore, in thiol-norbornene reactions there is no homopolymerization or chain growth between strained norbornene groups and the gelation is much faster [22]. Norbornene end groups are widely used in the modification of both natural (e.g., hyaluronic acid, alginate) and synthetic (e.g., polyethylene glycol) polymers owing their fast reactivity and cytocompatibility. Norbornene-functionalized polymers can be rapidly converted into cell-laden hydrogels under physiologically relevant conditions and the crosslinking reaction did not affect the cell viability [10,23,24]. As the norbornene moieties are only reactive in the presence of active radical species, hydrogels bearing free norbornene groups can be explored to dynamically modulate the material properties and/or cell fate after hydrogel formation without cytotoxic effects for the embedded cells [25].

Recently, we reported on the development of photocrosslinkable methacrylate-modified pectin for the bioprinting of cell-responsive tissue constructs for skin applications [26]. Although bioprinted RGD-functionalized pectin hydrogels support the spreading of embedded dermal fibroblasts and *de novo* deposition of endogenously synthesized ECM, cell-mediated hydrogel remodeling is limited by the lack of protease degradable sites. This study describes for the first time the synthesis of norbornene-functionalized pectin macromers for thiol-ene photopolymerization reactions. Macromers are rapidly converted into cell-instructive hydrogels through one-pot, photo-click reaction with a monocysteine RGD integrin binding peptide and a biscysteine matrix-metalloproteinase (MMP)-cleavable peptide as crosslinker. These new polymer-peptide conjugates are rapidly prepared in the presence of cells through an efficient thiol-norbornene reaction, providing sites for cell attachment and cellular-driven remodeling of the hydrogel network. This photo-click reaction also affords spatiotemporal control over the hydrogel formation and allows easy manipulation of biophysical and biochemical cues presented to the embedded cells. The proposed novel pectin hydrogel system allows the one-step formation of chemically defined cell-laden hydrogels capable of supporting the *in vitro* formation of full-thickness skin.

2. Materials and methods

2.1. Synthesis of norbornene functionalized pectin

The norbornene-functionalized pectin (NorPEC) was synthetized through the reaction with carbic anhydride (CA, Acros Organics) in dimethyl sulfoxide (DMSO). Prior to synthesis, low methoxyl citrus pectin (Classic CU701, 86% galacturonic acid unit content and 37% degree of methylation, Herbstreith & Fox, Neuenbürg, Germany) was purified [16] and converted into tetrabutylammonium salt (PEC-TBA) for solubilization in organic solvents. Pectin was dissolved in ultrapure water at 1 wt%, the Dowex 50 W proton exchange resin (Acros Organics) was added to the solution (3.5 g resin per 1 g polymer) and allowed to exchange under vigorous agitation for 3 h. The solution was centrifuged to remove the resin, filtered (0.20 μm) and neutralized to pH 6.50 with tetrabutylammonium (TBA, Sigma-Aldrich). The solution was subsequently frozen, lyophilized and stored at -20 °C. For the synthesis of NorPEC, PEC-TBA was dissolved in anhydrous DMSO at 1 wt% and CA added at 1-fold molar excess to hydroxyl groups in the polymer backbone. The solution reacted under vigorous agitation and inert (N_2) atmosphere at room temperature for 1 h. After this, the solution was immediately transferred to dialysis (MWCO 3500, Spectra/Por®, SpectrumLabs) with sodium chloride for 3 days, followed by purification with deionized water for additional 2 days. Then, the solution was treated with activated charcoal (1 g charcoal per 1 g of polymer, Sigma-Aldrich) for 1 h, centrifuged (60 000 rcf, Beckman Avanti J-26XP) and filtered (0.20 μm). Finally, the pH was adjusted to 7.00 with sodium hydroxide (0.1 M), the solution frozen and the polymer recovered by lyophilization. The product was dissolved in deuterated water (D_2O, Euriso-top) containing 3-(trimethylsilyl)propionic-2,2,3,3-d 4 acid sodium salt (TSP-d_4, Euriso-top) as internal standard ($\delta = 0$ ppm) and analyzed by ^{1}H NMR using a 400 MHz spectrometer AVANCE III (Bruker).

2.2. Formation and characterization of photocrosslinked hydrogels

For the fabrication of hydrogels, NorPEC macromer (2.5 wt%) was dissolved in 0.9 wt% NaCl containing the photoinitiator VA-086 (0.25 wt%, Wako Chemicals), the peptide crosslinker CGPQG↓IWGQC (4–6 mM, arrow indicates enzymatically cleavable site, Genscript) and the cell-adhesive peptide ligand CGGGGRGDSP (0–2 mM, underline indicates cell-adhesion motif, Genscript) at

desired concentrations. After dissolution, the solution was pipetted on the top of a glass slide treated with SigmaCote (Sigma-Aldrich) to prevent attachment of the gel, covered by a treated glass side with 500 μm spacers and polymerized under UV light (365 nm, RoHS) at 7 mW/cm^2 for 20 s.

To characterize the shear modulus, hydrogels were soaked in PBS at 37 °C for 24 h and the samples (Ø = 4 mm) tested in a humidified environment at physiological temperature (37 °C) using a strain-controlled Kinexus Pro rheometer (Malvern). Both frequency sweeps (0.01–10 Hz at 1% strain) and strain sweeps (0.1–100% at 0.1 Hz) were performed on swollen samples (30% compression) to ensure that all measurements were representative of the linear viscoelastic regime.

The swelling ratio was determined by soaking freeze-dried hydrogel samples in PBS (0.5 mL) at 37 °C for 24 h. Hydrogel samples were collected, the superficial excess of water was gently removed with a tissue paper, and the swollen weight determined. Swelling ratio (q) was determined by dividing the weight of hydrated hydrogel by its initial dry weight.

The degradation of MMP-degradable NorPEC hydrogels was evaluated in the presence of Type II Collagenase (385 U/mg, Worthington Biochemical). Immediately after photopolymerization hydrogels were frozen and lyophilized to determine the initial weight (W_I). Dry samples were hydrated overnight in Hanks' Balanced Salt solution (HBSS) at 37 °C, followed by incubation in 0.5 mL HBSS containing Type II Collagenase at 2 U/mL, which corresponds to the collagenase concentration during the initial phase of the wound healing process [27]. At specific time periods, samples were removed from the solution, washed with ultrapure water, frozen and lyophilized to determine the final weight (W_F) after degradation. The degradation was expressed in percentage of the weight loss compared to the initial dry mass and determined using the following equation:

$$Degradation \, (\%) = \frac{W_I - W_F}{W_I} \times 100 \qquad (1)$$

To determine the amount of non-bound RGD peptide during photopolymerization, hydrogels were incubated in 0.5 mL PBS at 37 °C for 24 h and the supernatant collected. The amount of released peptide in PBS was quantified by reversed phase chromatography (Merck-Hitachi HPLC) equipped with a detector at 220 nm. Samples were run at 1 mL/min on a LiChroCART 250–4 C18 column, eluting with 0.065/0.05 v/v% trifluoroacetic acid in water/acetonitrile, respectively. The calibration curve for peptide quantification was obtained using the peptide dissolved in PBS at different concentrations (0–2 mM).

2.3. 3D cell embedding within hydrogels, cell viability and morphology analysis

Human neonatal dermal fibroblasts (hNDFs) isolated from human neonatal foreskin samples (Coriell Institute for Medical Research, USA) were cultured in DMEM supplemented with 10% fetal bovine serum (FBS, Gibco), antibiotics (100 U/mL penicillin and 100 μg/mL streptomycin, Sigma-Aldrich) and amphotericin B (2.5 mg/L, Sigma-Aldrich). Cells were cultured in 5% CO$_2$ at 37 °C in tissue culture polystyrene flasks. To characterize the behaviour of hNDFs within MMP-degradable NorPEC hydrogels, cells (passage 6 to 9) were trypsinized before reaching confluence (70–80%) using 0.05 wt% trypsin/ethylenediamine tetraacetic acid (EDTA) solution (Sigma-Aldrich) and centrifuged at 1200 rpm for 5 min. The cell pellet was suspended and added to the NorPEC gel precursor solution at a final density of 1×10^7 cells/mL. Cellular gel precursor solution (20 μL) was pipetted between SigmaCote-treated glass slides and cell-laden hydrogels obtained by UV photopolymeriza-

tion. At predetermined time periods (day 1, 7 and 14), cell-laden hydrogels were collected and characterized for their metabolic activity, cell viability and cell morphology.

Metabolic activity of cells embedded with NorPEC hydrogels was assessed by the resazurin assay. Hydrogels were incubated in DMEM medium containing 20 v/v% resazurin sodium salt (Sigma-Aldrich) for 2 h at 37 °C. Samples were measured using a microplate reader (Synergy MX, Biotek) at 530 nm (excitation) and 590 nm (emission).

Cell viability was measured using the Live/Dead cytotoxicity kit (Life Technologies) according to the manufacturer instructions. Briefly, cell-laden hydrogels were incubated in phenol red-free DMEM media (Life Technologies) containing 1 μM calcein and 4 μM ethidium homodimer for 30 min. Cell-laden hydrogels were imaged on a laser scanning microscope (CLSM, Leica TCS-SP5 AOBS, Leica Microsystems).

The morphology of cells within NorPEC hydrogels was observed by immunofluorescence staining for F-actin and nuclei. Cell-laden hydrogels were fixed in 4 v/v% paraformaldehyde (PFA, Electron Microscopy Sciences) in HBSS (Life Technologies) for 20 min, followed by extensive washing with HBSS. Samples were incubated overnight with phalloidin/Alexa Fluor® 488 (1:40, Molecular Probes-Invitrogen) for F-actin staining, followed by incubation with Hoechst (Life Technologies) for nuclei staining for 45 min. Then, samples were extensively rinsed and imaged on a laser scanning microscope (CLSM, Leica TCS-SP5 AOBS, Leica Microsystems).

2.4. Matrix metalloproteinases (MMPs) secretion by gelatin zymography

To determine the expression of MMP-2 and MMP-9 from fibroblasts embedded within hydrogels of different stiffness, cell culture supernatants were collected at different time periods (day 1 and 3) and the levels compared to culture media in the absence of cell-laden hydrogels. After collection, conditioned media was centrifuged to remove cell debris and the total protein content in lysates of cells recovered from the hydrogels quantified by the DC protein assay (BioRad). Sample volumes were adjusted to yield equivalent total cell protein contents, loaded into gelatin-SDS polyacrylamide gels, and run in 1 × Tris-Glycine SDS running buffer at 80 V (Mini Protean Tetra Cell system, BioRad). Following electrophoresis, gels were washed in 2 v/v% Triton X-100 to remove the SDS and incubated with MMP substrate buffer for 16 h at 37 °C. Then, gels were washed and stained with Coomassie Brilliant Blue R-250 (Sigma Aldrich). The activity of MMPs was visualized by clear bands in the stained gels and compared to molecular weight and standards. The gel was washed with distilled water, scanned using the GS-800 Calibrated Densiometer (Bio-Rad), and the activity of MMPs estimated by densitometric analysis (Quantity One, Bio-rad).

2.5. Formation of full-thickness skin using cell-instructive pectin hydrogel

The skin equivalent was constructed by the photopolymerization of MMP-degradable NorPEC gel precursor solution loaded with fibroblasts (1×10^7 cells/mL), as previously described. Cell-laden hydrogels were cultured submerged for 7 days. After this time period, cell line keratinocytes (HaCaT) were seeded onto the fibroblast-loaded hydrogel (5×10^5 cells/cm^2), left to attach for 2 h and cultured submerged for 7 days. Then, the constructs were cultured at the air-liquid interface (ALI culture) for either 14 days or 28 days [28]. Culture medium was changed every two days in submerged culture and daily in ALI culture.

2.6. Histological and immunofluorescence analysis

Skin equivalents were rinsed with HBSS, fixed in 4 v/v% paraformaldehyde in HBSS for 30 min and extensively washed. Then, samples were embedded in paraffin, sectioned onto 6 μm slides and representative sections were stained for Hematoxylin/ Eosin (H&E) and Masson's Trichrome using routine protocols. The sections were mounted on coverslips and observed with an optical microscope. For immunofluorescence analysis, deparaffinized sections were subjected to heat-induced antigen retrieval, permeabilized with 0.25 v/v% Triton X-100 (Sigma-Aldrich) in PBS and rinsed with PBS, followed by blocking and overnight incubation with primary antibodies at 4 °C (Table S1). Then, sections were rinsed and incubated with secondary antibodies for 1 h at room temperature, following extensive washing. After mounting, the sections were observed in a microscope (AxioImager Z1, Carl Zeiss). Negative controls were performed by replacing the primary antibody with blocking buffer.

2.7. Statistical analysis

Statistical analyses were performed in the GraphPad Prism 7.0 software. All experimental data are reported as the mean ± standard deviation (SD) of at least three individual samples. Unless stated, the non-parametric Mann–Whitney test was applied with 95% confidence interval and statistically significant differences marked with $p < .05$ (∗), $p < .01$ (∗∗), $p < .001$ (∗∗∗) and $p < .0001$ (∗∗∗∗).

3. Results and discussion

3.1. Synthesis of norbornene-functionalized pectin macromers for thiol-ene photopolymerization

In thiol-ene photopolymerization, the reaction kinetics, the extent of conversion and the structure of the polymer network are determined by the reactivity between thiols and carbon–carbon double bonds (referred to as alkenes), which in turn depends on the alkene chemical structure [29]. Among the variety of alkene functional groups capable of reacting with thiols, it is well-established that strained (norbornene) and electron-rich alkenes (e.g., vinyl ether) react faster than electron-poor alkenes [30]. Specifically, the strained norbornene functional group has received increased attention for thiol-ene reactions as it follows exclusively step-growth mechanism and displays extremely high reactivity, which can be explained by the relief of ring strain after thiyl radical addition, absence of abstractable hydrogens and stereoelectronic effects [29,31]. In this work, pectin was functionalized with norbornene functional groups for the fabrication of cell-laden hydrogels through thiol-ene click reaction in the presence of a low concentration type I photoinitiator and UV light. Norbornene-functionalized pectin was synthetized via an esterification reaction between pectin and carbic anhydride (CA) in DMSO for 1 h at room temperature (Fig. 1a). Secondary hydroxyl groups of the polymer served as nucleophiles for reaction with CA, without compromising the water-solubility of modified polymer. The reaction was performed in organic solvents to overcome the limited solubility of CA in aqueous solutions and its pH dependence [32]. This strategy allows the neutralization of carboxylate groups with sodium ions to improve the water-solubility of synthetized macromers and to prevent spontaneous ionic gelation of photocrosslinked hydrogels in culture medium mediated by positively charged calcium ions (Supplementary Fig. S1). Pectin was firstly converted to its tetra-butylammonium salt (PEC-TBA) for solubilization in organic solvents via reaction with the Dowex ion-exchange resin, followed by neutralization with tetrabutylammonium (TBA), as can be seen

in the ^{1}H NMR spectra by the appearance of new peaks corresponding to the butyl groups (3.20, 1.66, 1.38, and 0.96 ppm) (Fig. 1b, Supplementary Fig. S2). Then, the lipophilic PEC-TBA was dissolved in anhydrous DMSO and reacted with CA under a N_2 atmosphere, yielding norbornene-functionalized pectin (NorPEC), as confirmed by ^{1}H NMR analysis through the appearance of new peaks (6.12–6.37 ppm) of vinyl protons on the norbornene functionality (Fig. 1b, Supplementary Fig. S3). The product was purified through dialysis against sodium chloride to ensure complete removal of the TBA via neutralization of the carboxylate groups into the sodium salt form. Further product purification was performed with activated charcoal and centrifugation to remove any unreacted CA and potential byproducts (Supplementary Fig. S4). The extent of norbornene substitution was determined to be 20.0 ± 0.6% through ^{1}H NMR analysis by comparing the integral values corresponding to norbornene protons (6.12–6.37 ppm) and native protons in the polymer backbone (3.82–4.43 ppm). Higher substitution can be achieved by changing either the reaction time or the CA content (Table S2). The reproducibility and robustness of the chemical reaction was confirmed by performing independent synthesis of norbornene-functionalized pectin, followed by ^{1}H NMR analysis (Supplementary Fig. S5). Compared to alternative strategies for norbornene-functionalization of natural polymers (e.g., gelatin, hyaluronic acid), which are performed under aqueous alkaline buffers (pH 8, 6 h, 50 °C) to ensure CA dissolution [32] or using di-tert-butyl dicarbonate coupling chemistry in DMSO (20 h, 45 °C) [23], the modification procedure previously described presents several advantages, such as (i) prevents the addition of catalysts, (ii) precludes the pH adjustment during the reaction, (iii) proceeds at room temperature, and (iv) significantly reduces the reaction time (1 h).

3.2. Formation and characterization of thiol-ene click pectin hydrogels

Biomimetic polymer-peptide hydrogels with MMP-cleavable peptide crosslinks are widely used as provisional matrices for tissue regeneration because they allow for localized cell-driven remodeling at the pericellular space, resembling the dynamic nature of ECM [7]. By simply altering the protease specific peptide crosslinker it was shown that engineered hydrogels differentially respond to MMPs secreted by distinct cell types, allowing for cell-specific invasion within the gel network and controllable cell responses [33,34]. In this work, enzymatically degradable, cell-instructive pectin hydrogels were prepared via a fast UV photoinitiated thiol-ene reaction between a peptide crosslinker sensitive to cell-secreted proteases (CGPQGIWGQC) flanked with biscysteine and the norbornene groups of NorPEC in the presence of VA-086 as a water-soluble photoinitiator (Fig. 2). To mimic the cell-mediated remodeling of natural skin ECM, the protease sensitive sequence GPQG↓IWGQ, derived from the sequence GPQG↓IAGQ found in type I collagen, was covalently incorporated into the polymer backbone. This peptide sequence was selected due to its susceptibility to cleavage by a wide range of MMPs (e.g., 1, 2, 3 and 9) secreted by several cell types involved in skin wound healing, including fibroblasts and keratinocytes [35,36], thus providing a substrate for cell degradation. After 20 s of UV photopolymerization, the biscysteine MMP-degradable peptide become part of the crosslinked hydrogel, allowing for local network degradation and determining both biophysical and biochemical properties. The mono-cysteine peptide CGGGGRGDSP (fibronectin-derived adhesion ligand based on RGD sequence) was also incorporated within the hydrogels as a pendant moiety, via one-pot reaction during gel formation, to provide integrin-mediated cell adhesion and cell-matrix crosstalk [10]. Although the physical adsorption of native integrin-binding proteins and biomolecules onto biomaterials can contribute to a more robust signaling, the hydrophilic nature of
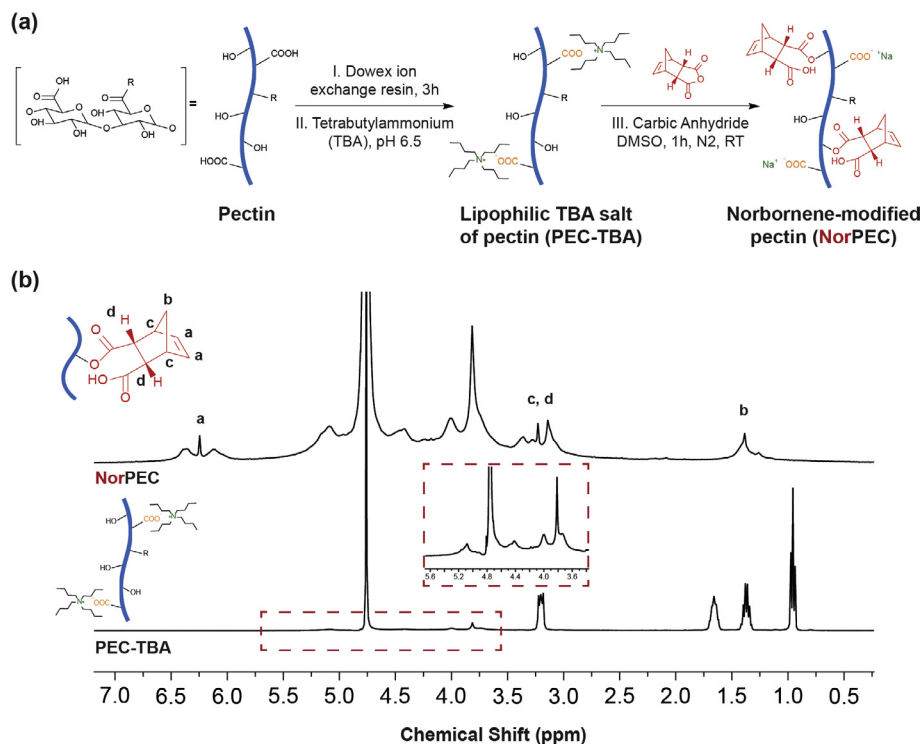
Fig. 1. Synthesis and characterization of pectin derivatives for thiol-ene photopolymerization. (a) Synthesis of norbornene-functionalized pectin (NorPEC) macromer from PEC-TBA through the coupling of norbornene groups (shown in red) to secondary alcohols on pectin (R denotes substituting group on carboxylic acid moiety: NH_2 or OCH_3). (b) ^1H NMR spectra (D_2O, 400 MHz) of NorPEC after 1 h reaction with carbic anhydride in DMSO and PEC-TBA after 3 h treatment with Dowex ion exchange resin and neutralization with tetrabutylammonium. Insert shows the native protons in pectin backbone.
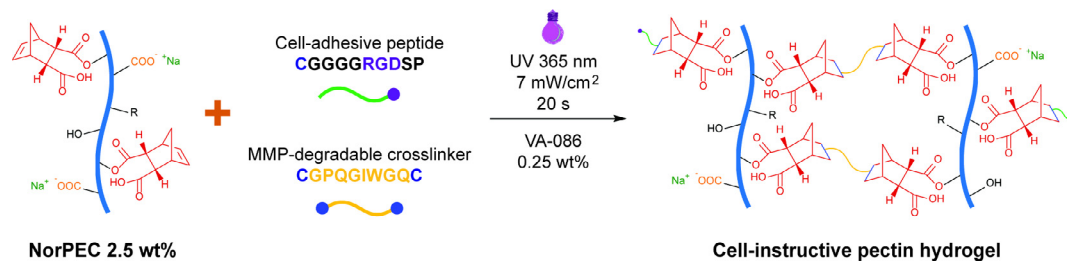

Fig. 2. Schematic illustration of photocrosslinking and biofunctionalization of click NorPEC hydrogels via UV light photoinitiated thiol-ene reaction of di-thiol MMP-degradable peptide (CGPQG↓IWGQC, arrow indicates enzymatically cleavable site) and norbornene groups on NorPEC. Mono-thiol cell-adhesive peptide (CGGGGRGDSP, underline indicates cell-adhesion motif) is tethered to the norbornene groups during the photopolymerization, providing pendant sites for cell-anchorage.

hydrogels strongly reduces this phenomenon, limiting cell adhesion both *in vitro* and *in vivo* [37,38]. A recent work with unmodified calcium-crosslinked pectin hydrogels prepared at different concentrations (1%, 2% and 4%) showed that macrophages seeded onto the hydrogel surfaces fail to adhere, though the hydrogels adsorbed blood plasma proteins in a polymer concentration dependent manner [39]. Therefore, the introduction of cell-adhesive peptides into the backbone of hydrogel precursors, including pectin, is recognized as an efficient strategy to promote cell adhesion. VA-086 was selected as photoinitiator owing to its strong absorbance at 365 nm and enhanced biocompatibility compared to the commonly used Irgacure 2959 [40]. We took advantage of the orthogonality and ultrahigh reactivity of norbornene moiety toward thiol-ene reaction to reduce the concentration of photoinitiator to 0.25 wt%. This concentration is significantly lower than the ones typically applied in radical-mediated polymerization (1.0–1.5 wt %), preventing the formation of macroscopic air bubbles within the hydrogel due to the N_2 generation [41,42].

In order to closely mimic key features of the ECM, hydrogel mechanical properties and biological functions should be tailored on relevant time scales by the user or the cells. There are several approaches to tailor the rheological properties of photocrosslink-able hydrogels, such as varying the crosslinking time, light intensity, polymer fraction, crosslinker content or the degree of alkene substitution. Increasing the polymer fraction enhances the number of alkene groups available for reaction, potentially leading to increased RGD-peptide conjugation. Similarly, increasing the crosslinking time/light intensity could lead to a similar outcome as the UV dose to which hydrogels are subjected is higher. Both strategies often result in altered ligand density between hydrogels, influencing the hydrogel properties and cell fate [10,43]. In this study, the crosslinking time, light intensity, polymer fraction and norbornene functionalization were maintained constant and the hydrogel crosslinking density was tailored by varying the content of MMP-peptide crosslinker. To evaluate the ability to precisely adjust the rheological properties, hydrogels were prepared with

varying bulk concentration of MMP-peptide crosslinker (4, 5 and 6 mM), while maintaining constant the concentration of polymer (2.5 wt%) and RGD peptide (2 mM). As shown in Fig. 3a, the rheological properties on the swollen state are dependent on the concentration of MMP-cleavable peptide used during the photopolymerization, with the shear elastic moduli varying

Fig. 3. Physical and mechanical properties of MMP-degradable NorPEC hydrogels. (a) Influence of MMP-cleavable peptide concentration on the storage modulus (G') of photocrosslinked hydrogels. (b) Swelling of hydrogels upon overnight incubation in PBS. (c) *In vitro* degradation of hydrogels prepared with varying contents of MMP-degradable peptide in the presence of collagenase type II.

between 70.03 ± 10.39 and 446.75 ± 35.66 Pa. Results show that higher MMP-cleavable peptide content increased the crosslink density and consequently the elastic modulus. To confirm such observations, the equilibrium mass swelling ratio of hydrogels was determined after 24 h of incubation in PBS (Fig. 3b). It was found that the swelling ratio decreases as the concentration of MMP-cleavable peptide increases, which correlates with the formation of a highly entangled and more crosslinked network. These data indicate that the elastic modulus and swelling of low polymer fraction hydrogels can be tailored via modulation of MMP-degradable peptide content, which is in agreement with previous works [25].

Enzymatically degradable hydrogels sensitive to the action of MMPs are of particular interest for tissue regeneration because proteases play a key role in numerous biological processes during development and morphogenesis, including ECM remodeling, wound healing and angiogenesis [44,45]. To confirm that thiol-ene hydrogels are susceptible to enzymatic degradation by collagenase type II, hydrogels with varying elastic moduli were incubated with the enzyme at a physiologically relevant concentration found during the wound healing [27] and their change in mass was determined as a function of time. It was found that all hydrogel formulations are sensitive to collagenase degradation and that the extent of degradation is dependent on the crosslinking density (Fig. 3c). Hydrogels crosslinked with 4 mM of MMP-cleavable peptide were completely degraded after 3 h of incubation, while hydrogels with 5 mM of MMP-cleavable peptide remained stable in solution for 5 h of incubation. In contrast, highly crosslinked hydrogels (6 mM MMP-sensitive peptide) maintained structural integrity throughout the assay, clearly showing a crosslinking density-dependent degradation. Control hydrogels incubated in HBSS buffer alone exhibited minimal mass loss after 9 h of incubation (Supplementary Fig. S6), indicating that the degradation is specifically triggered by enzymatic stimuli. Due to the recent introduction of pectin-based hydrogels in the field of tissue engineering, evidence regarding the mechanisms underlying the clearance/degradation of pectin from the human body is still scarce. Since the degradation of pectin is mediated by several pectinases (e.g., pectate lyases, polygalacturonases) absent in the human body, the degradation of pectin hydrogels by collagenase could facilitate the polymer clearance upon implantation. As pectin polymer chains are crosslinked by the MMP-sensitive peptide, it is expected that the cleavage of the hydrogel network into soluble pectin chains facilitates the degradation/clearance of pectin via interaction with the complex proteolytic environment (e.g., physiological enzymes, cell-secreted proteases, pH and temperature) found *in vivo*.

3.3. Chemically defined cell-instructive pectin hydrogels promote 3D cell attachment and spreading

A major challenge when using natural polymers as cellularized ECM-analogues relies on the difficulty of designing hydrogels with independently tunable biochemical and biophysical properties, an important feature to precisely modulate cell functions [46,47]. To decouple the influence of crosslinking density (MMP-cleavable peptide) from ligand density (RGD peptide) on the behavior of embedded dermal fibroblasts, cell-laden hydrogels were produced with varying ligand density (0–2 mM), but using constant polymer concentration (2.5 wt%) and MMP-cleavable peptide content (5 mM). Live/Dead analysis showed that the majority of the cells remained alive after 7 days of culture, with marked differences on the morphology and distribution within the gel network (Fig. 4a). The incorporation of RGD peptide conferred adhesiveness to the otherwise inert pectin network and was necessary to promote cell adhesion and spreading within the hydrogels. Fibroblasts cultured within RGD-functionalized hydrogels showed elongated
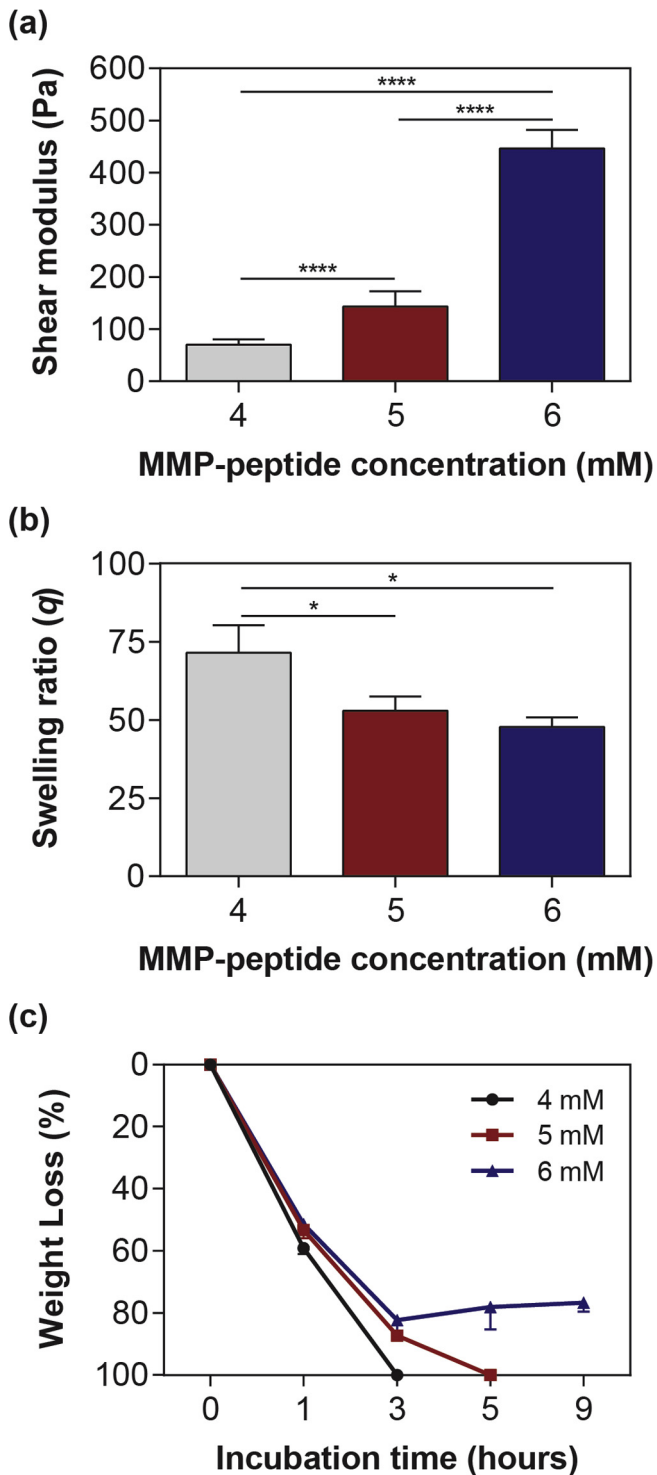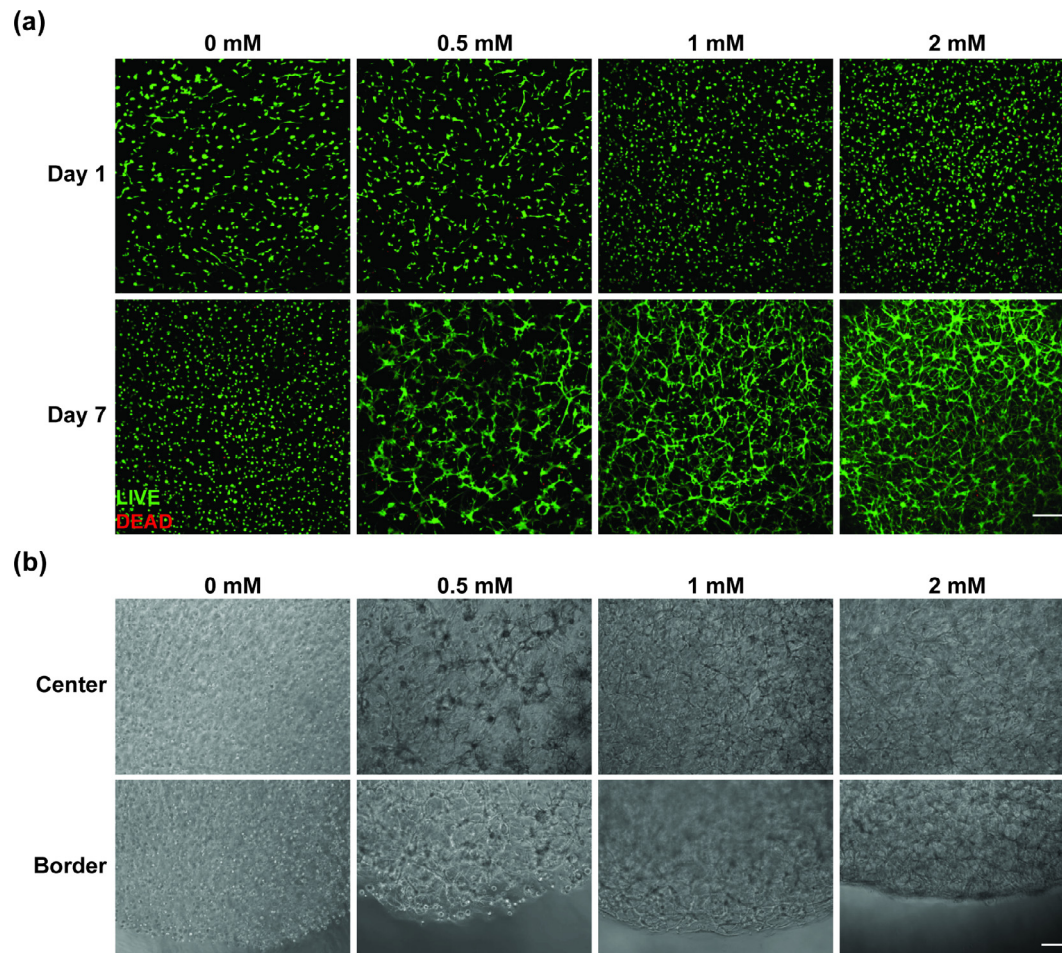
(a)

(b)

Fig. 4. Influence of RGD peptide on dermal fibroblasts encapsulated within MMP-degradable NorPEC hydrogels. (a) Representative Live/dead images of fibroblasts embedded within 2.5% NorPEC hydrogels (5 mM MMP peptide, 20 s UV), showing the effect of bulk RGD concentration (0–2 mM) on cell viability and distribution within the hydrogels at day 7 (scale bar: 200 μm). (b) Bright-field images showing the influence of RGD peptide content on the spreading of fibroblasts in the center and periphery of hydrogels at day 7 of culture (scale bar: 100 μm).

morphology with major differences on the spreading and elongation as a function of the bulk RGD content. At day 7, cells within hydrogels containing 0.5 mM RGD displayed heterogeneous spreading at both the center and periphery of the gels, while fibroblasts embedded within hydrogels with higher concentrations of RGD peptide (1 and 2 mM) were uniformly spread throughout the gel network (Fig. 4b). In the absence of RGD, cells remained mostly round without spreading and lacking cell-cell contacts, though they remained metabolically active (Supplementary Fig. S7). These results indicate that the peptide density determines the extent of cell spreading, which could be easily controlled by changing the bulk concentration of RGD peptide during the thiolene reaction. The influence of ligand density (RGD peptide) on cell spreading within thiol-ene 3D hydrogels has been investigated using several cell types [48–50]. For instance, Bott et al. [49] showed that dermal fibroblasts embedded within MMP-degradable PEG hydrogels lacking cell-adhesion sites or containing the non-biologically active RDG peptide sequence remain round, while the tethering of RGD peptide promoted cell adhesion and spreading. In another work, Kyburz et al. [48] reported that the adhesivity of MMP-degradable PEG hydrogels determines the spreading and migration of hMSCs in 3D. At 0 and 0.001 mM CRGDS concentrations embedded hMSCs remained round, while increasing the CRGDS concentration to 1.0 mM promoted a significant increase in cell spreading, elongation and migration. These authors hypothesized that increased network adhesivity facilitates cell attachment and spreading, providing the necessary traction for

cells to migrate. In this work, RGD was used at a concentration of 2.0 mM in order to maximize the number of adhesion sites and promote uniform cell spreading within the hydrogel.

To investigate the influence of matrix stiffness on cell behavior, fibroblasts were embedded within MMP-degradable hydrogels (2.5 wt%, 2 mM RGD) of varying moduli. Adding the MMP-cleavable peptide at three different contents (4, 5 and 6 mM) resulted in the formation of hydrogels with low, medium and high crosslinking densities, respectively. Fibroblasts cultured within all hydrogel formulations remained metabolically active throughout 14 days of culture (Supplementary Fig. S8) and extensively spread within the hydrogel network (Fig. 5a). Major differences between the hydrogels were observed regarding the time required for cells to spread, cell compaction and hydrogel contraction. At early time points (day 1), fibroblasts were round in stiffer hydrogels (5 and 6 mM MMP) and displayed elongated morphology in loosely cross-linked gels (4 mM MMP). At day 3, extensive cell spreading and elongation was observed in hydrogels with low and medium crosslinking density, while in hydrogels with high crosslinking density the majority of cells only start spreading, with few protrusions. At later time points (day 7), cells extensively spread within all hydrogels independently of the crosslinking density (Supplementary Fig. S9). Fibroblasts embedded within MMP-degradable pectin hydrogels formed 3D interconnected multicellular networks and assumed a spindle-shaped morphology, characteristic of fibroblasts cultured within 3D environments [49]. Although MMP-degradable hydrogels supported extensive cell spreading,
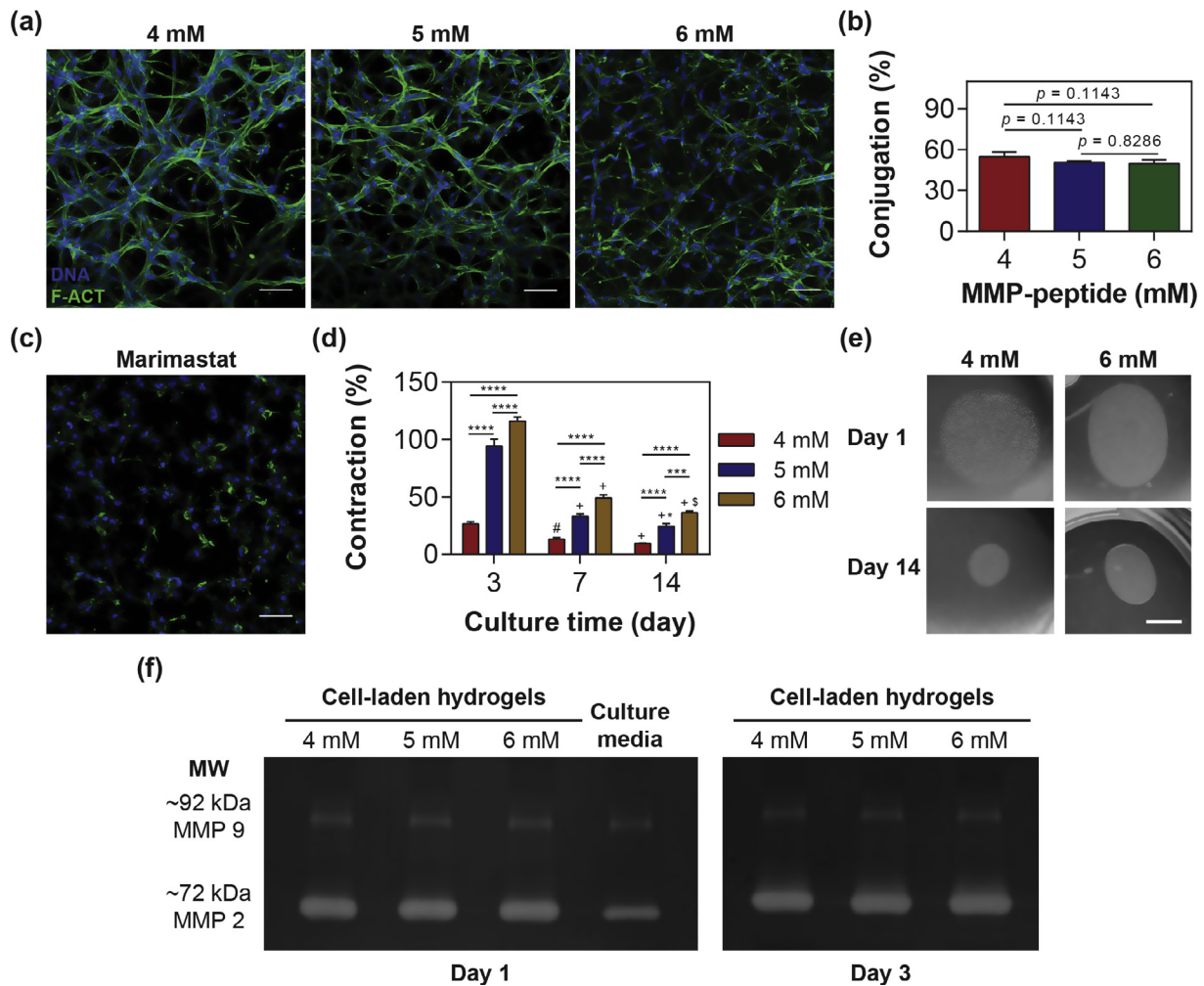
Fig. 5. Cell encapsulation of dermal fibroblasts within MMP-degradable NorPEC hydrogels. (a) Representative confocal microscopy images detailing the influence of MMP-peptide content (4, 5 and 6 mM MMP-cleavable peptide, 2.5% NorPEC, 2 mM RGD peptide, 20 s UV) on the morphology and spatial distribution of fibroblasts stained for DAPI (blue) and F-actin (green) at day 14 (scale bar: 50 μm). (b) Influence of bulk MMP-degradable peptide content on the conjugation efficiency of RGD-peptide during photopolymerization. (c) Representative confocal microscopy images of fibroblasts cultured within NorPEC hydrogels (2.5%, 6 mM MMP, 2 mM RGD) in medium containing 50 μM of MMP-inhibitor Marimastat at day 7 (scale bar: 50 μm). (d) Effect of MMP-peptide content on the contraction of hydrogels during the culture period. Results are expressed as a percentage of area reduction compared to day 1. (e) Photographs showing the appearance of low and highly crosslinked hydrogels at day 1 and 14 of culture (scale bar: 2.5 mm). (f) Gelatin-zymograms of conditioned media collected at day 1 and 3. Data from contraction assays were analyzed using two-way ANOVA with Tukey's multiple comparisons test ($^{***}p < .001$, $^{****}p < .0001$); compared to day 3: $^{+}p < .0001$, $^{\#}$ $p < .001$; compared to day 7: $^{*}p < .01$, $^{\$}p < .001$.

confocal images showed that cells cultured within stiffer hydrogels exhibit more pronounced compaction (Supplementary Fig. S9), suggesting that the extent of cell compaction correlates with the hydrogel stiffness. To prove that differences in fibroblasts spreading and morphology were not a result of changes in the content of tethered RGD peptide during the thiol-ene photopolymerization, HPLC analysis was carried out to confirm that the conjugation efficiency was comparable between all hydrogel formulations (4 mM: 54.91 ± 3.40%; 5 mM: 50.77 ± 0.90%; 6 mM: 49.61 ± 2.92%), as shown in Fig. 5b and further confirmed using a fluorescently labeled RGD-peptide (Supplementary Fig. S10). Results show that fibroblasts require more time to spread and remodel denser hydrogels, even in presence of MMP-cleavable peptide crosslinkers, due to the physical constrains imposed by the matrix. Our observations are in agreement with a previous work reporting a significant reduction on the percentage of hMSCs capable of elongate and migrate within thiol-ene MMP-degradable PEG hydrogels of increased crosslinking density [48].

As the rate of cell spreading, elongation and migration in 3D is dictated by both biochemical and biophysical cues [48], cell-laden hydrogels with varying crosslinking density were also cultured in

the presence of a broad-spectrum MMP inhibitor (Marimastat) to assess whether cell spreading was exclusively dependent on MMP-mediated hydrogel degradation (Supplementary Fig. S11). Fibroblasts displayed an elongated morphology within loosely crosslinked hydrogels throughout the 14 days of culture period, even in the presence of MMP inhibitor, suggesting that cells spread essentially by an MMP-independent mechanism (e.g., defects in the gel network). In contrast, cells embedded within medium or highly crosslinked hydrogels incubated with Marimastat failed to spread and remained mostly spherical with a few elongated cells located near the hydrogel surface. F-actin staining further confirmed that cells embedded within highly crosslinked hydrogels remained isolated and presented only minor protrusions (Fig. 5c), indicating that cells are only able to overcome the physical barrier of the matrix by enzymatic cleavage. Therefore, cell elongation within cell-degradable pectin hydrogels is determined not only by MMP-mediated degradation, but also by the hydrogel stiffness. For hydrogels with low crosslinking density (G' = 70.03 ± 10.39 Pa), the stiffness was found to be a key parameter determining cell elongation, while in stiffer hydrogels (G' > 143.09 ± 29.70 Pa) cell spreading was driven by MMP-mediated degradation. In a previous

work using fully interpenetrating networks made of collagen-I and RGD-functionalized alginate with embedded dermal fibroblasts, it was found that cells fully spread within hydrogels of low storage modulus (50 Pa), but remained spherical when encapsulated in hydrogels of both intermediate (320 Pa) and high (1200 Pa) stiffness [51], which is in agreement to our observations regarding the effects of matrix stiffness on the response of dermal fibroblasts. The incorporation of MMP-cleavable peptides as part of the pectin hydrogel network allows embedded fibroblasts to locally degrade the surrounding matrix, which is essential to create space for spreading and elongation. Although cells require more time to degrade the matrix of highly crosslinked matrices, they are also able to fully spread in stiffer 3D hydrogels (446.80 ± 35.66 Pa), forming interconnected cellular networks throughout the hydrogel.

Fibroblasts play a key role during the healing of deep wounds, being involved in ECM synthesis, deposition and remodeling, while exerting forces towards wound contraction [52]. The contraction of cell-laden hydrogels was monitored during the culture period to determine whether the crosslinking density can be used to control dimensional changes of hydrogel network (Fig. 5d,e). After three days of culture, only hydrogels crosslinked with 4 mM MMP-cleavable peptide shrank when compared to day 1, while at day 7 a significant reduction on the hydrogel's area was observed for all compositions. Loosely crosslinked hydrogels (4 mM MMP) displayed the highest shrinkage degree, reaching 9.7% of their initial area at day 14. Hydrogels with medium and high crosslinking degree reached 24.3% and 36.4% of their initial area at the same culture time. Embedded fibroblasts were able to pull on the matrix and contract it in a matrix stiffness-dependent manner, as a result of contractile forces involved in cell attachment, elongation and migration [53]. These results showed that hydrogel contraction by dermal fibroblasts is linked to matrix stiffness, with higher stiffness correlating with both increased structural integrity and lower contraction degree. Thus, by using MMP-degradable pectin hydrogels of varying stiffness it's possible to modulate the contractility of embedded fibroblasts and associated matrix deformation.

During the healing of skin wounds, fibroblasts, keratinocytes, endothelial cells and inflammatory cells secrete a broad range of MMPs, which expression and activation is tightly regulated [54,55]. MMPs play a pivotal role throughout the process, namely by changing the properties of the wound matrix to allow cell migration and new ECM deposition. In order to evaluate whether fibroblasts embedded within MMP-degradable hydrogels secrete relevant MMPs for remodeling, the activity levels of two ubiquitous gelatinases (MMP-2 and MMP-9) involved in skin wound healing [54], were determined in culture medium by gelatin zymography at different culture times (Fig. 5f). Zymography analysis clearly showed that cells produced MMP-2 (72 kDa) and MMP-9 (92 kDa), with higher expression of MMP-2. It was also found that the activity of MMP-2 increased from day 1 to day 3 of culture, which corresponds to the time period that fibroblasts start spreading within the gel network. Characteristic bands of MMP-9 were detected at low levels in conditioned media, indicating that embedded fibroblasts mostly express MMP-2, which is in agreement to previous works with dermal fibroblasts cultured in 3D hydrogels [49].

3.4. Thiol-ene click pectin hydrogels support full-thickness skin formation

To demonstrate the potential of the MMP-degradable pectin hydrogels for skin repair and regeneration, dermal fibroblasts were embedded within pectin hydrogels of medium crosslinking density (2.5% NorPEC, 2 mM RGD, 5 mM MMP), cultured for 1 week and subsequently seeded with keratinocytes. After submerged culture

for additional 1 week, cell-laden hydrogels were exposed to the air-liquid interface to promote the stratification of epidermis and characterized by both histological and immunofluorescence analysis. Histological analyses depicted in Fig. 6a clearly show that cell-instructive pectin hydrogels supported the *in vitro* formation of full-thickness skin, with morphological resemblance to the human skin. H&E staining (Fig. 6a) showed that the dermal compartment is uniformly populated with elongated dermal fibroblasts, while a well-defined epidermis was formed on the top of the fibroblast-laden hydrogel. Keratinocytes formed a dense epidermal tissue after 14 days of ALI culture with marked differences on cell morphology as a function of their location in the epidermis. Basal keratinocytes in the close proximity to the dermal-like layer display a cuboidal shape, while most of the cells at the epidermis-air interface present a flattened morphology, which is characteristic of the differentiation and stratification of keratinocytes [56]. A higher number of flattened keratinocytes at the surface of the constructs could be observed at day 28 of ALI culture compared to day 14 (Supplementary Fig. S12a). Notably, the thickness of the epidermis-like layer (∼120 μm) is within the range of native human epidermis, which varies in the interval 60–150 μm, depending on the location in the human body [57]. Masson's tri-chrome staining (Fig. 6b) revealed that fibroblasts were secreting collagen, a key ECM component of skin tissue, with more intense blue staining (increased deposition) from day 14 to day 28 of ALI culture (Supplementary Fig. S12b). Immunohistological analysis also showed the presence of specific markers associated to epidermal differentiation and proliferation, including cytokeratin (Fig. 6c) and Ki67 (Supplementary Fig. S13), respectively. The presence of Ki67 proliferation marker mainly in the suprabasal layers of epidermis correlates with the differentiation state of the keratinocytes, as in native skin only keratinocytes in the *stratum basale* maintain proliferative activity [56]. To confirm that the presence of fibroblasts is limited to the dermal compartment, sections were stained against vimentin, a cytoskeletal protein characteristic of fibroblasts (Fig. 6d). No cell invasion across dermal and epidermal layers was observed, since the presence of cytokeratin- and vimentin-positive cells was limited to the epidermal and dermal layers, respectively. Key characteristic markers of ECM production in dermal compartment were also identified such as collagen type-I (Fig. 6e) and fibronectin (Fig. 6f), indicating that fibroblasts were secreting essential ECM components for new dermal tissue formation. Although these results clearly demonstrate that protease-degradable pectin hydrogels support the *in vitro* formation of skin equivalents, a limitation of the present study relies on the use of immortalized keratinocyte cell line (HaCaT) to generate the epidermal layer instead of primary keratinocytes. It's well recognized that immortalized keratinocytes undergo gradual loss of cell phenotype and function throughout passaging and culture, which can delay or even compromise the stratification and terminal differentiation [58]. However, we anticipate that the use of primary keratinocytes can potentially address this issue.

In a future work we will focus on the detailed characterization of the performance of MMP-sensitive pectin hydrogels in skin formation and adhesion to biological tissues. The ability of MMP-degradable pectin hydrogels to support the *in vitro* skin formation will be compared to MMP-insensitive pectin hydrogels (e.g., dithio-threitol (DTT), non-degradable CGDQGIAGFC peptide crosslinker) and standard constructs for skin tissue engineering (e.g., collagen, alginate) to elucidate the benefits of the proposed hydrogel. The adhesion of hydrogels to the surrounding biological tissues is challenging in wound healing as it requires the establishment of chemical bonds between the hydrogel and the tissue surface for sufficient bonding strength. *In situ* photopolymerizable hydrogels are particularly advantageous for wound healing as they can be formed under clinically safe 365 nm light irradiation, conform to
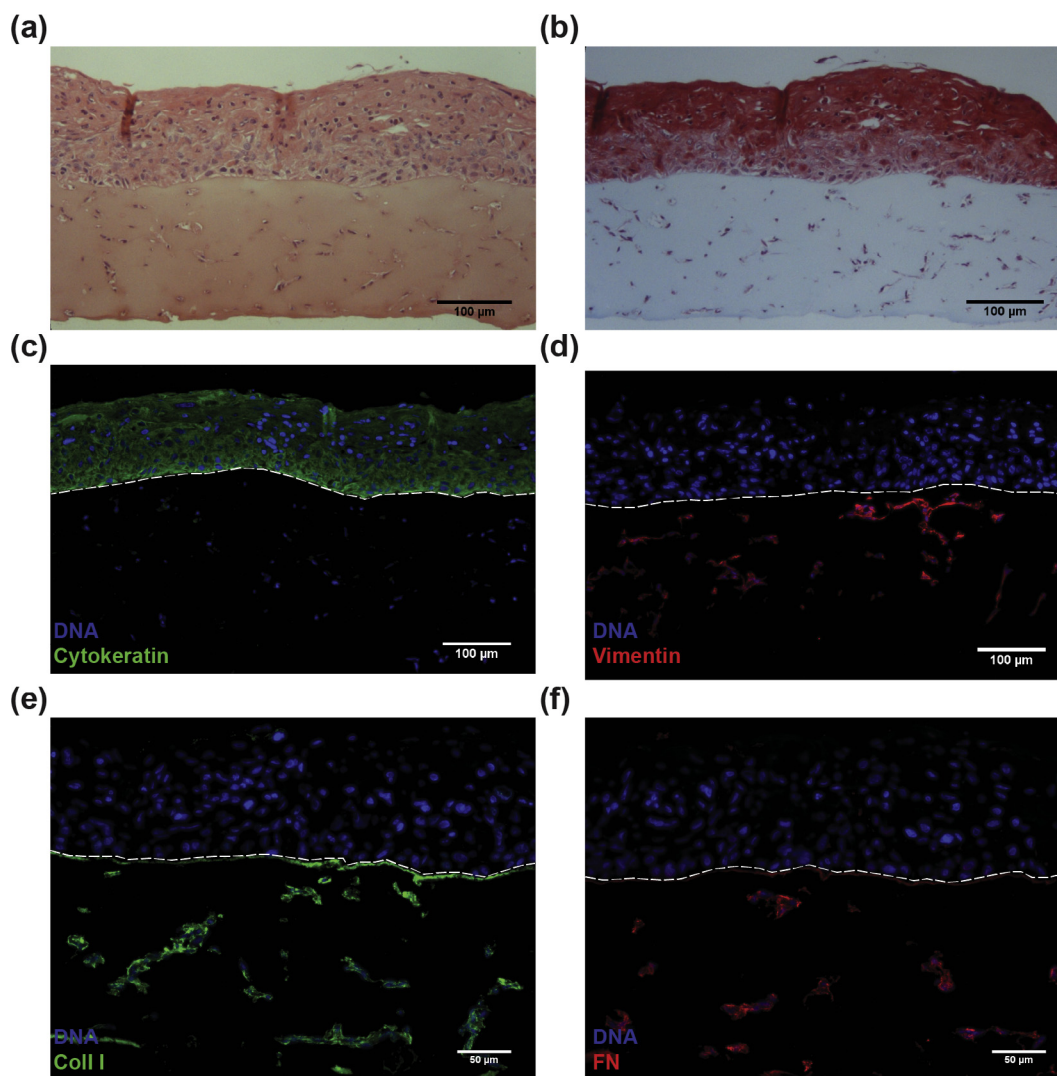
Fig. 6. Histological and morphological characterization of skin equivalents formed using the protease-degradable pectin hydrogels after 14 days of differentiation at the air-liquid interface. (a) Hematoxylin & eosin and (b) Masson trichrome staining's showing the histology of skin equivalents. Immunostaining of paraffin embedded samples using antibodies directed against (c) cytokeratin (keratinocytes), (d) vimentin (fibroblasts), (e) collagen type-I (Coll I) and (f) fibronectin (FN). Dash line delineates the interface between the dermal and epidermal layers.

the wound bed, and depending on the chemical composition, can enhance the interaction with the tissue surface promoting better integration [59]. The developed MMP-sensitive pectin hydrogel exhibits key properties for wound healing such as fast gelation (Supplementary Fig. S14) and the ability to promote cell spreading, ECM deposition and *in vitro* skin formation. Pectin hydrogels also contain multiple domains that bind do cell-surface receptors, with potential to promote subsequent cell attachment and tissue integration. In addition, the carboxylic groups present in the pectin backbone can also contribute for tissue adhesion through interaction with amino groups [39]. In case of poor hydrogel adhesion and integration, the chemical versatility of pectin allows for easy modification with functional groups (e.g., aldehydes) capable of reacting with the amino groups present on the tissue surface. Alternative biomimetic strategies to improve the tissue adhesion can also be translated to pectin hydrogels, including the functionalization with mussel adhesive proteins (MAPs) containing the amino acid 3,4-dihydroxyphenylalanine (DOPA). Through oxidative crosslinking or metal chelation, the catechol moiety in DOPA amino acid chain covalently crosslinks both to itself and to biologically relevant nucleophiles (e.g., primary amines and thiols),

allowing better tissue adhesion and improving hemostasis [60]. Due to the poor yield in the isolation and purification of MAPs, nature-inspired adhesive hydrogels have been mostly designed by incorporating DOPA-based peptides and simplified DOPA alternatives such as dopamine and catechol functional groups [61–63]. Mussel-inspired functionalization represents an attractive strategy to improve the wet adhesion of hydrogels with particular interest for *in situ* skin tissue engineering.

4. Conclusion

A simple, fast and robust method for the synthesis of norbornene-functionalized pectin was developed and applied for the fabrication of cell-laden MMP-cleavable hydrogels through photoinitiated thiol-ene reaction. Step-growth pectin hydrogels were rapidly formed upon exposure to UV light for very short irradiation times, without compromising the viability of embedded dermal fibroblasts. By selecting suitable MMP-degradable peptide crosslinkers and pendant cell-adhesive peptides, biofunctional hydrogels were engineered with varying levels of crosslinking density, resulting in distinct biological responses. Embedded

fibroblasts displayed elongated morphology and less compaction in more permissive hydrogels, contracting the matrix in a higher extent. Cell-instructive hydrogels with embedded dermal fibroblasts and seeded with keratinocytes supported the *in vitro* formation of full-thickness skin resembling the architecture and morphology of human skin. Two distinct regions corresponding to the dermal and epidermal layers were formed, showing the presence of specific markers associated to proliferation and ECM deposition. This versatile hydrogel system allows for independent tuning of biochemical and biophysical cues of the gel network, allowing the fabrication of chemically defined 3D matrices from pectin as a natural polymer. Overall, this study demonstrates the potential of novel biofunctionalized, click pectin hydrogels for skin tissue engineering applications.

Acknowledgements

Appendix A. Supplementary data

Supplementary data associated with this article can be found, in the online version, at https://doi.org/10.1016/j.actbio.2017.11.016.

References

[1] S.A. Eming, P. Martin, M. Tomic-Canic, Wound repair and regeneration: mechanisms, signaling, and translation, Sci. Transl. Med. 6 (2014). 265sr6.

[2] R.F. Pereira, C.C. Barrias, P.L. Granja, P.J. Bartolo, Advanced biofabrication strategies for skin regeneration and repair, Nanomedicine (Lond.) 8 (2013) 603–621.

[3] R.F. Pereira, P.J. Bartolo, Traditional therapies for skin wound healing, Adv. Wound Care (New Rochelle) 5 (2016) 208–229.

[4] A.S. Klar, S. Guven, T. Biedermann, J. Luginbuhl, S. Bottcher-Haberzeth, C. Meuli-Simmen, M. Meuli, I. Martin, A. Scherberich, E. Reichmann, Tissue-engineered dermo-epidermal skin grafts prevascularized with adipose-derived cells, Biomaterials 35 (2014) 5065–5078.

[5] G. Sun, X. Zhang, Y.I. Shen, R. Sebastian, L.E. Dickinson, K. Fox-Talbot, M. Reinblatt, C. Steenbergen, J.W. Harmon, S. Gerecht, Dextran hydrogel scaffolds enhance angiogenic responses and promote complete skin regeneration during burn wound healing, Proc. Natl. Acad. Sci. U. S. A. 108 (2011) 20976–20981.

[6] C. Huang, H. Orbay, M. Tobita, M. Miyamoto, Y. Tabata, H. Hyakusoku, H. Mizuno, Proapoptotic effect of control-released basic fibroblast growth factor on skin wound healing in a diabetic mouse model, Wound Repair Regen. 24 (2016) 65–74.

[7] K.B. Fonseca, P.L. Granja, C.C. Barrias, Engineering proteolytically-degradable artificial extracellular matrices, Prog. Polym. Sci. 39 (2014) 2010–2029.

[8] E. Jabbari, J. Leijten, Q. Xu, A. Khademhosseini, The matrix reloaded: the evolution of regenerative hydrogels, Mater. Today 19 (2016) 190–196.

[9] M.V. Tsurkan, K. Chwalek, S. Prokoph, A. Zieris, K.R. Levental, U. Freudenberg, C. Werner, Defined polymer-peptide conjugates to form cell-instructive starPEG-heparin matrices in situ, Adv. Mater. 25 (2013) 2606–2610.

[10] B.D. Fairbanks, M.P. Schwartz, A.E. Halevi, C.R. Nuttelman, C.N. Bowman, K.S. Anseth, A versatile synthetic extracellular matrix mimic via thiol-norbornene photopolymerization, Adv. Mater. 21 (2009) 5005–5010.

[11] K.B. Fonseca, D.B. Gomes, K. Lee, S.G. Santos, A. Sousa, E.A. Silva, D.J. Mooney, P. L. Granja, C.C. Barrias, Injectable MMP-sensitive alginate hydrogels as hMSC delivery systems, Biomacromolecules 15 (2014) 380–390.

[12] T. Tokatlian, C. Cam, T. Segura, Porous hyaluronic acid hydrogels for localized nonviral DNA delivery in a diabetic wound healing model, Adv. Healthc. Mater. 4 (2015) 1084–1091.

[13] F. Munarin, M.C. Tanzi, P. Petrini, Advances in biomedical applications of pectin gels, Int. J. Biol. Macromol. 51 (2012) 681–689.

[14] F. Munarin, S.G. Guerreiro, M.A. Grellier, M.C. Tanzi, M.A. Barbosa, P. Petrini, P. L. Granja, Pectin-based injectable biomaterials for bone tissue engineering, Biomacromolecules 12 (2011) 568–577.

[15] P. Coimbra, P. Ferreira, H.C. de Sousa, P. Batista, M.A. Rodrigues, I.J. Correia, M. H. Gil, Preparation and chemical and biological characterization of a pectin/chitosan polyelectrolyte complex scaffold for possible bone tissue engineering applications, Int. J. Biol. Macromol. 48 (2011) 112–118.

[16] S.C. Neves, D.B. Gomes, A. Sousa, S.J. Bidarra, P. Petrini, L. Moroni, C.C. Barrias, P.L. Granja, Biofunctionalized pectin hydrogels as 3D cellular microenvironments, J. Mater. Chem. B 3 (2015) 2096–2108.

[17] F. Munarin, P. Petrini, M.C. Tanzi, M.A. Barbosa, P.L. Granja, Biofunctional chemically modified pectin for cell delivery, Soft Matter 8 (2012) 4731.

[18] P.M. Kharkar, K.L. Kiick, A.M. Kloxin, Designing degradable hydrogels for orthogonal control of cell microenvironments, Chem. Soc. Rev. 42 (2013) 7335–7372.

[19] R.F. Pereira, P.J. Bártolo, 3D photo-fabrication for tissue engineering and drug delivery, Engineering 1 (2015) 090–112.

[20] M.W. Tibbitt, A.M. Kloxin, L. Sawicki, K.S. Anseth, Mechanical properties and degradation of chain and step polymerized photodegradable hydrogels, Macromolecules 46 (2013) 2785–2792.

[21] J.J. Roberts, S.J. Bryant, Comparison of photopolymerizable thiol-ene PEG and acrylate-based PEG hydrogels for cartilage development, Biomaterials 34 (2013) 9969–9979.

[22] C.C. Lin, C.S. Ki, H. Shih, Thiol-norbornene photo-click hydrogels for tissue engineering applications, J. Appl. Polym. Sci. 132 (2015) 41563.

[23] W.M. Gramlich, I.L. Kim, J.A. Burdick, Synthesis and orthogonal photopatterning of hyaluronic acid hydrogels with thiol-norbornene chemistry, Biomaterials 34 (2013) 9803–9811.

[24] R.M. Desai, S.T. Koshy, S.A. Hilderbrand, D.J. Mooney, N.S. Joshi, Versatile click alginate hydrogels crosslinked via tetrazine–norbornene chemistry, Biomaterials 50 (2015) 30–37.

[25] K.M. Mabry, R.L. Lawrence, K.S. Anseth, Dynamic stiffening of poly(ethylene glycol)-based hydrogels to direct valvular interstitial cell phenotype in a three-dimensional environment, Biomaterials 49 (2015) 47–56.

[26] R. Pereira, A. Sousa, C. Barrias, P. Bártolo, P. Granja, P023 A cell-responsive, photocrosslinkable bioink for extrusion bioprinting of 3D hydrogel constructs, Eur. Cell. Mater. 33 (2) (2017).

[27] M.S. Agren, C.J. Taplin, J.F. Woessner Jr., W.H. Eaglstein, P.M. Mertz, Collagenase in wound healing: effect of wound age and type, J Invest Dermatol 99 (1992) 709–714.

[28] P. Gangatirkar, S. Paquet-Fifield, A. Li, R. Rossi, P. Kaur, Establishment of 3D organotypic cultures using human neonatal epidermal cells, Nat. Protocols 2 (2007) 178–186.

[29] T.M. Roper, C.A. Guymon, E.S. Jönsson, C.E. Hoyle, Influence of the alkene structure on the mechanism and kinetics of thiol-alkene photopolymerizations with real-time infrared spectroscopy, J. Polym. Sci., Part A: Polym. Chem. 42 (2004) 6283–6298.

[30] C.E. Hoyle, C.N. Bowman, Thiol-ene click chemistry, Angew. Chem. Int. Ed. Engl. 49 (2010) 1540–1573.

[31] B.H. Northrop, R.N. Coffey, Thiol-ene click chemistry: computational and kinetic analysis of the influence of alkene functionality, J. Am. Chem. Soc. 134 (2012) 13804–13817.

[32] Z. Mũnoz, H. Shih, C.-C. Lin, Gelatin hydrogels formed by orthogonal thiol–norbornene photochemistry for cell encapsulation, Biomater. Sci. 2 (2014) 1063–1072.

[33] M. Bracher, D. Bezuidenhout, M.P. Lutolf, T. Franz, M. Sun, P. Zilla, N.H. Davies, Cell specific ingrowth hydrogels, Biomaterials 34 (2013) 6797–6803.

[34] A.K. Jha, K.M. Tharp, S. Browne, J. Ye, A. Stahl, Y. Yeghiazarians, K.E. Healy, Matrix metalloproteinase-13 mediated degradation of hyaluronic acid-based matrices orchestrates stem cell engraftment through vascular integration, Biomaterials 89 (2016) 136–147.

[35] J. Patterson, J.A. Hubbell, Enhanced proteolytic degradation of molecularly engineered PEG hydrogels in response to MMP-1 and MMP-2, Biomaterials 31 (2010) 7836–7845.

[36] A.A. Tandara, T.A. Mustoe, MMP- and TIMP-secretion by human cutaneous keratinocytes and fibroblasts–impact of coculture and hydration, J. Plast. Reconstr. Aesthet. Surg. 64 (2011) 108–116.

[37] J.A. Rowley, G. Madlambayan, D.J. Mooney, Alginate hydrogels as synthetic extracellular matrix materials, Biomaterials 20 (1999) 45–53.

[38] T.T. Lee, J.R. García, J.I. Paez, A. Singh, E.A. Phelps, S. Weis, Z. Shafiq, A. Shekaran, A. del Campo, A.J. García, Light-triggered in vivo activation of adhesive peptides regulates cell adhesion, inflammation and vascularization of biomaterials, Nat. Mater 14 (2015) 352–360.

[39] P.A. Markov, N.S. Krachkovsky, E.A. Durnev, E.A. Martinson, S.G. Litvinets, S.V. Popov, Mechanical properties, structure, bioadhesion, and biocompatibility of pectin hydrogels, J. Biomed. Mater. Res. A 105 (2017) 2572–2581.

[40] A.D. Rouillard, C.M. Berglund, J.Y. Lee, W.J. Polacheck, Y. Tsui, L.J. Bonassar, B.J. Kirby, Methods for photocrosslinking alginate hydrogel scaffolds with high cell viability, Tissue Eng. Part C Meth. 17 (2011) 173–179.

[41] P. Occhetta, R. Visone, L. Russo, L. Cipolla, M. Moretti, M. Rasponi, VA-086 methacrylate gelatine photopolymerizable hydrogels: a parametric study for

highly biocompatible 3D cell embedding, J. Biomed. Mater. Res. A 103 (2015) 2109–2117.

[42] E.E. Coates, C.N. Riggin, J.P. Fisher, Photocrosslinked alginate with hyaluronic acid hydrogels as vehicles for mesenchymal stem cell encapsulation and chondrogenesis, J. Biomed. Mater. Res. A 101 (2013) 1962–1970.

[43] S.P. Zustiak, R. Durbal, J.B. Leach, Influence of cell-adhesive peptide ligands on poly(ethylene glycol) hydrogel physical, mechanical and transport properties, Acta Biomaterialia 6 (2010) 3404–3414.

[44] C. Bonnans, J. Chou, Z. Werb, Remodelling the extracellular matrix in development and disease, Nat. Rev. Mol. Cell. Biol. 15 (2014) 786–801.

[45] A. Page-McCaw, A.J. Ewald, Z. Werb, Matrix metalloproteinases and the regulation of tissue remodelling, Nat. Rev. Mol. Cell Biol. 8 (2007) 221–233.

[46] R. Cruz-Acuna, A.J. Garcia, Synthetic hydrogels mimicking basement membrane matrices to promote cell-matrix interactions, Matrix Biol. 57–58 (2017) 324–333.

[47] J. Patterson, M.M. Martino, J.A. Hubbell, Biomimetic materials in tissue engineering, Mater. Today 13 (2010) 14–22.

[48] K.A. Kyburz, K.S. Anseth, Three-dimensional hMSC motility within peptide-functionalized PEG-based hydrogels of varying adhesivity and crosslinking density, Acta Biomater. 9 (2013) 6381–6392.

[49] K. Bott, Z. Upton, K. Schrobback, M. Ehrbar, J.A. Hubbell, M.P. Lutolf, S.C. Rizzi, The effect of matrix characteristics on fibroblast proliferation in 3D gels, Biomaterials 31 (2010) 8454–8464.

[50] M.P. Schwartz, B.D. Fairbanks, R.E. Rogers, R. Rangarajan, M.H. Zaman, K.S. Anseth, A synthetic strategy for mimicking the extracellular matrix provides new insight about tumor cell migration, Integr. Biol. (Camb.) 2 (2010) 32–40.

[51] C. Branco da Cunha, D.D. Klumpers, W.A. Li, S.T. Koshy, J.C. Weaver, O. Chaudhuri, P.L. Granja, D.J. Mooney, Influence of the stiffness of three-dimensional alginate/collagen-I interpenetrating networks on fibroblast biology, Biomaterials 35 (2014) 8927–8936.

[52] P. Bainbridge, Wound healing and the role of fibroblasts, J. Wound Care 22 (407–8) (2013) 410–412.

[53] M. Eastwood, R. Porter, U. Khan, G. McGrouther, R. Brown, Quantitative analysis of collagen gel contractile forces generated by dermal fibroblasts and the relationship to cell morphology, J. Cell. Physiol. 166 (1996) 33–42.

[54] M.P. Caley, V.L. Martins, E.A. O'Toole, Metalloproteinases and wound healing, Adv. Wound Care (New Rochelle) 4 (2015) 225–234.

[55] R. Lobmann, A. Ambrosch, G. Schultz, K. Waldmann, S. Schiweck, H. Lehnert, Expression of matrix-metalloproteinases and their inhibitors in the wounds of diabetic and non-diabetic patients, Diabetologia 45 (2002) 1011–1016.

[56] A. Baroni, E. Buommino, V. De Gregorio, E. Ruocco, V. Ruocco, R. Wolf, Structure and function of the epidermis related to barrier properties, Clin. Dermatol. 30 (2012) 257–262.

[57] M.J. Koehler, T. Vogel, P. Elsner, K. Konig, R. Buckle, M. Kaatz, In vivo measurement of the human epidermal thickness in different localizations by multiphoton laser tomography, Skin Res. Technol. 16 (2010) 259–264.

[58] N. Maas-Szabowski, A. Starker, N.E. Fusenig, Epidermal tissue regeneration and stromal interaction in HaCaT cells is initiated by TGF-alpha, J. Cell Sci. 116 (2003) 2937–2948.

[59] Y. Yang, J. Zhang, Z. Liu, Q. Lin, X. Liu, C. Bao, Y. Wang, L. Zhu, Tissue-integratable and biocompatible photogelation by the imine crosslinking reaction, Adv. Mater. 28 (2016) 2724–2730.

[60] M. Shin, S.-G. Park, B.-C. Oh, K. Kim, S. Jo, M.S. Lee, S.S. Oh, S.-H. Hong, E.-C. Shin, K.-S. Kim, S.-W. Kang, H. Lee, Complete prevention of blood loss with self-sealing haemostatic needles, Nat. Mater. 16 (2017) 147–152.

[61] R. Wang, J. Li, W. Chen, T. Xu, S. Yun, Z. Xu, Z. Xu, T. Sato, B. Chi, H. Xu, A biomimetic mussel-inspired ε-poly-l-lysine hydrogel with robust tissue-anchor and anti-infection capacity, Adv. Funct. Mater. 27 (2017). 1604894-n/a.

[62] C. Fan, J. Fu, W. Zhu, D.-A. Wang, A mussel-inspired double-crosslinked tissue adhesive intended for internal medical use, Acta Biomater. 33 (2016) 51–63.

[63] B.P. Lee, C.-Y. Chao, F.N. Nunalee, E. Motan, K.R. Shull, P.B. Messersmith, Rapid gel formation and adhesion in photocurable and biodegradable block copolymers with high DOPA content, Macromolecules 39 (2006) 1740–1748.